IOP Conf. Series: Materials Science and Engineering **418** (2018) 012101 doi:10.1088/1757-899X/418/1/012101

A New Hybrid Bead with Post-stretching Method to Effectively Control Spring-back for Advanced High Strength Steel

Yueqian (Victor) Jia[1], **Chao Pu**[1], **Feng Zhu**[1], **Ken Schmid**[2], **Yu-wei Wang**[1]

[1] Advanced Engineering & Applications Laboratory, AK Steel Coporation, Dearborn, MI 48120
[2] General Motors Corporation, 30500 Mound Rd, Warren, MI 48092

Corresponding author: Yu-wei Wang, Email address: yu-wei.wang@aksteel.com

Abstract
Spring-back issues are critical in stamping procedures for advanced high strength steel. The spring-back can be comprehensively controlled by applying a newly designed hybrid bead to effectuate a post-stretching process in a U-channel part forming. Finite element forming simulation is applied in a cross-section to evaluate and optimize the hybrid bead performance, using DP980. A specific post-stretching die with the optimized hybrid bead was manufactured and applied to demonstrate the performances. Excellent spring-back control and material restricting effect were observed in the stamping results. Both effects of clamping force and post-stretching amount are systematically studied, using 1.2mm DP980 and CP1180 AHSS sheets. Significant tonnage reduction was achieved, comparing to the original stinger bead design. An analytical solution was also applied to predict the same process with good correlation.

KEYWORDS: Advanced High Strength Steel, Post-stretching, Stinger Bead, Hybrid Bead, Bead Optimization, Finite Element Simulation, Analytical Solution

1. Introduction
Spring-back is one of the critical issues in advanced high strength steel (AHSS) applications, frequently causing defects in cold formed parts. AHSSs' higher level of stress and consequent elastic recovery in forming process severely hinder the applications comparing to mild steel [1,2]. Spring-back can be categorized into: a) angular change, b) sidewall curl, and c) twist based on part geometric changes.

A typical U-bending process is widely applied in sheet metal forming, where the blank experiences a complicated loading history. Loading conditions of bending, un-bending, and stretching are all included during the forming process. Sidewall curl, as a severe cross-sectional spring-back, often appears after tool removal. Finite element (FE) simulation can usually give reliable results correlating with the actual stamped and sprung-back parts, and it has been applied for many different parts and forming scenarios [3–12]. It can also investigate material behaviors in different scales [13–16].

An important method to control cross-sectional spring-back in sheet metal forming for AHSS is to increase plastic deformation by applying stretch bending process. Its effect on spring-back reduction has been studied experimentally and theoretically [17]. It would be more efficient to reduce spring-back if the stretching part is applied at the late stage of forming, known as post-stretching [3,18]. It has been extensively applied recently and proved effective especially for AHSS [19,20]. A stinger-typed bead was developed to lock the material during this procedure [21].

The objective of this manuscript is to further improve the spring-back controlling performance by optimize the post-stretching bead. FE method will be applied in the bead geometrical optimization process, based on an existed stinger-shaped bead. Experimental work will be conducted using a new post-stretching U-channel die, with the optimal bead incorporated. Multiple types of AHSSs will be applied. The effects of clamping force and post-stretching amount will be investigated, aiming at reducing the required machine tonnage. The experimental spring-back shapes would be digitally sketched for analyses, and also compared to analytical solutions.

2. Post-stretching Mechanism and Process

A post-stretching procedure is applied in the forming process to control the spring-back effect. A post-stretching bead is designed to fully lock the material flow when the drawing procedure is almost finished, exerting an external stretching force. The part will experience pure stretching after the bead engagement. The post-stretching bead is aligned with the punchline. The binder is divided into outer and inner binders, where the post-stretching bead is located at the inner binder. A 10% gap is retained by applying forces to stop blocks between the outer binder and the die/upper binder. Nitrogen spring cylinders are applied to assist implementing the post-stretching procedure. The post-stretching procedure is initiated when the forming is nearly completed. Two different scenarios are available with accommodating die/punch motions. Both of them can equivalently form the same part. They are described as follows.

a) The nitrogen spring cylinders are distributed underneath the inner binder to directly apply the clamping force to engage the post-stretching bead. The punch is supposed to be fixed during the entire stamping process. The binders and the die are supposed to move downward to form the part. The inner binder will be held stationary to form the post-stretching bead until the applied force exceeds the initial reaction force of the spring cylinders. The inner binder will move downward together with the outer binder and the die after bead engagement, to complete the rest of the part forming with a strong stretching.

b) The nitrogen spring cylinders are distributed underneath the outer binder. The die piece, known as the upper binder, remains stationary, as well as the outer binder after its closing. The punch is in motion to form the part. The inner binder will be driven by the machine to engage the post-stretching bead forming, while the outer binder remains stationary and is under the pressure of the nitrogen spring cylinders.

The scenario b) will be applied through this manuscript, including die design, experimental work and FE simulations.

3. FE Simulation for Bead Optimization

3.1. FE Model and Bead Geometries

The post-stretching bead plays a critical role in restricting the material flow, which would be the prerequisite to conduct the post-stretching procedure. A 2D symmetric cross-sectional FE model is established in Abaqus to optimize the bead shape, starting with an original stinger-type bead design. It consists of three micro ridges embossed on the inner binder (known as “teeth”) with slightly various trapezoidal shapes. Each of them has cross-sectional dimensions of approximately 0.5mm by 0.5mm. It has been manufactured and applied in an actual stamping plant before. The teeth would penetrate into the blank material after bead engagement, exerting a lateral force to restrict the material flow.

A modified bead design is described as follows. The middle tooth is moved to and embedded in the upper binder, staggering arranged between the other two teeth on the inner binder. Inversed shape of the middle tooth is debossed on the upper binder, opening two grooves as binder cavities. This design aims at generating a tiny waved-shape on the blank after bead engagement, along with material penetration

to synergistically enhance the material locking effect. A comparison between two designs is shown in Figure 1.

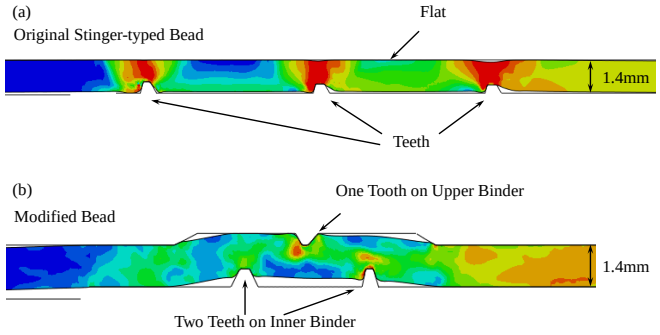

Figure 1 Comparison between geometries of (a) original stinger bead and (b) the modified bead. The contours represent the von-Mises equivalent stress. Both geometries are proportionally scaled.

The drawing process will be configured in the FE model. The outer and the upper binder are fixed in the model during the entire process. A concentrate force will be applied to the inner binder when the post-stretching procedure initiates. The magnitude of the concentrated force is defined as 2000N per unit length, which makes the teeth adequately intrude into the blank. The punch continues to move to the home position, finishing the entire drawing. The blank is then supposed to be under pure stretching in this stage, if the material flow restriction is strong enough. The mechanism is illustrated in Figure 2.

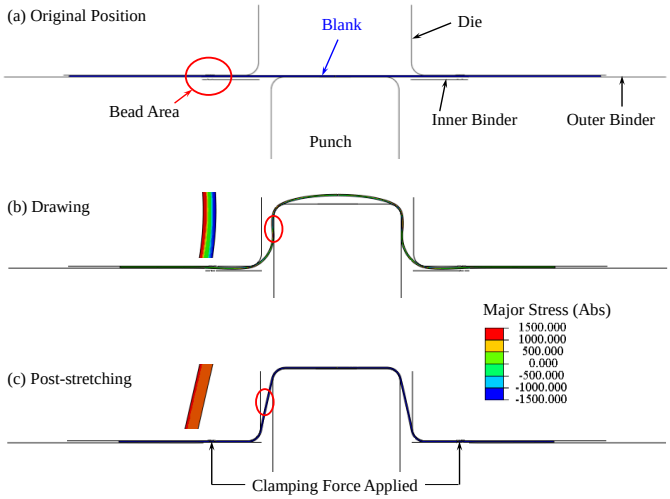

Figure 2 The stamping process with post-stretching included. (a) The original position right before stamping initiation, (b) the blank after pure-drawing process, and (c) the formed part after post-stretching. A magnified local area in sidewall is extracted in both subfigures (b) and (c), with a contour of absolute major stress.

This step can be modeled alternatively by simply restrict the horizontal displacement at the bead position. The external force is immediately generated when the post-stretching procedure initiates. It is considered as an ideal case under fully-lock situation. It can then be compared to the cases using post-stretching beads, for the purpose of bead performance evaluation.

The blank is defined by 4-node bilinear plane strain elements with reduced integration (CPE4R). Tools are all modeled as rigid bodies. A friction coefficient μ=0.08 is applied. An experimental 1.4mm

gauged DP980 is applied as an isotropic material hardening rule, with von-Mises yield criterion. The model is conducted by Abaqus explicit solver, and then transferred to spring-back analysis using Abaqus standard solver.

3.2. Bead Performance Evaluation

Strong stress difference is observed during the drawing process mainly due to the bending-dominated deformation mode and its bending-unbending history. The inner surface is generally under compressive loading while the outer is under tension, except for the lower die radius area where the stress conditions are inversed. The inner and outer surface in the wall area extends and retracts respectively after the recoveries of elastic strain without or with minimum post-stretching involved. However, the inner side stress condition can be altered into tension if the part is post-stretched to a relatively high strain level. Now both sides consistently retract due to their tension statuses, yielding only minimum spring-back.

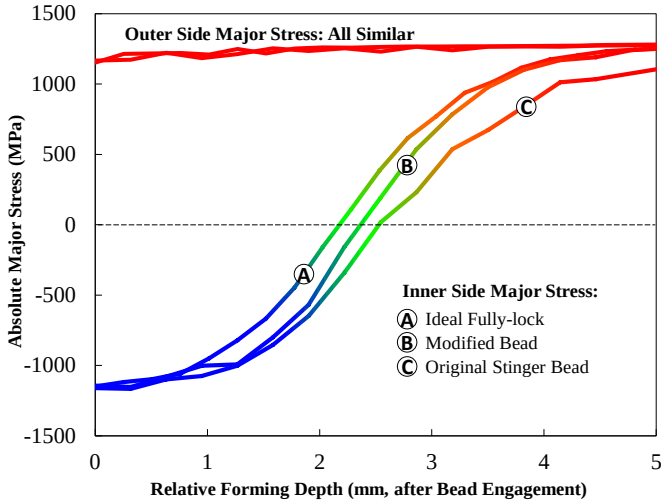

Figure 3 Stress evolution curves during the forming depth after bead engagement. The absolute major stresses are extracted from both inner and outer sides of the sidewall.

The evolution of sidewall stress difference during the post-stretching procedure can be illustrated in Figure 3. The shown contour indicates in-plane absolute major stress. Figure 3 compares the post-stretching performances among different circumstances: a) ideally locked, b) the modified bead design, and c) the original stinger-typed bead design. The converging rate of stress difference can be used to evaluate the bead performance. The fastest evolution would be under case a). It can be immediately seen that the case b), the modified bead design, has its inner stress evolutional curve coincided with the ideal case a). Therefore, the modified bead design can be considered an optimal.

4. Experimental Study of Post-stretching

4.1. Test Configuration and Objective

A lab-scale die was designed and manufactured for the post-stretching study, illustrated by Figure 4. The die is installed in SP225 Interlaken servo press machine located in AK Steel advanced engineering lab. The materials applied in this study are DP980 and CP1180, both are with 1.2mm gauge. A 100mm by 420mm rectangular blank is applied. A 20 Ton outer binder force is consistently applied for every case based on the combined pressure of the nitrogen spring cylinders.

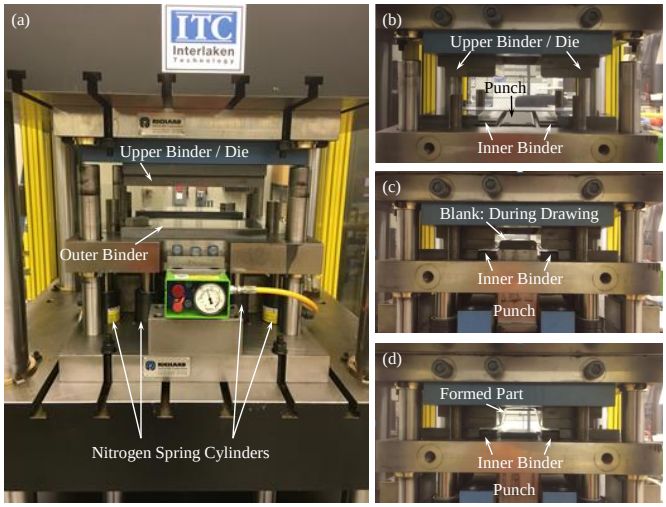

Figure 4 The manufactured die with the modified bead and post-stretching process incorporated. (a) Original position from the front view, (b) original position, (c) during pure-drawing procedure, and (d) after part formed from the side view.

4.2. Results and Analyses

A designed test matrix with their results in sidewall curl angle is illustrated in Figure 5 and Figure 6. It demonstrates and summarizes both effects of clamping force and post-stretching amount. It can be seen that the spring-back behavior of the given U-channel is well controlled after approaching an effective post-stretching amount of 7mm. Its effectiveness can be ensured if a minimum sufficient clamping force of 0.1Ton/mm or 0.175Ton/mm for DP980 or CP1180, respectively. No apparent blank sliding can be observed if the clamping force exceeds the given lower boundaries. Occurrences of both bead damage and blank slivering would be highly possible under this circumstance.

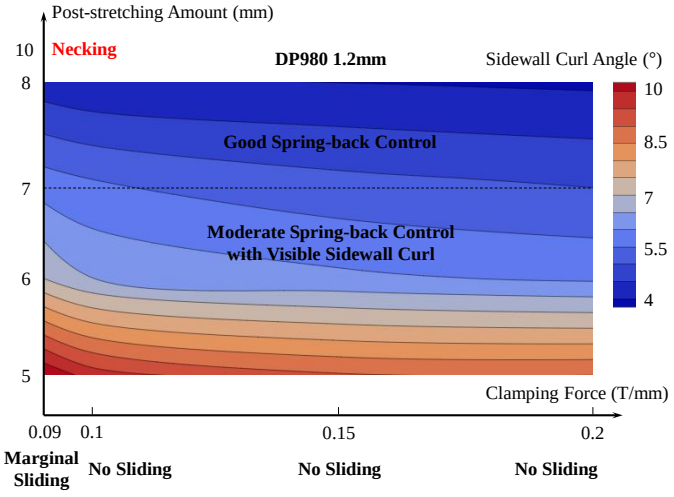

Figure 5 Contour of sidewall curl angles for 1.2mm DP980. A 0.1Ton/mm clamping force is considered minimally adequate. A 7mm effective post-stretching amount would be sufficient to control spring-back behavior.

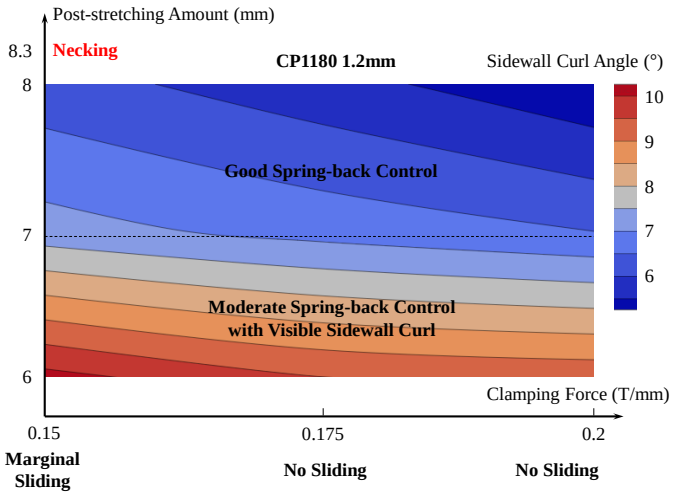

Figure 6 Contour of sidewall curl angles for 1.2mm CP1180. A 0.175Ton/mm clamping force is considered minimally adequate. A 7mm effective post-stretching amount would be sufficient to control spring-back behavior.

A few representative cases using the original stinger bead are compared to the optimized bead cases. Their results are shown in Figure 7. It can be immediately seen that its clamping effect is much less adequate than the optimized bead. A minimum clamping force of 0.2Ton/mm is required for DP980, which is 100% larger than the optimized bead case. The 100% clamping force increase (0.35Ton/mm) is still insufficient for fully restricting the material flow for CP1180, where apparent blank sliding is observed. A comparison of material sliding phenomena is depicted in Figure 7, between the original stinger bead and the optimized bead.

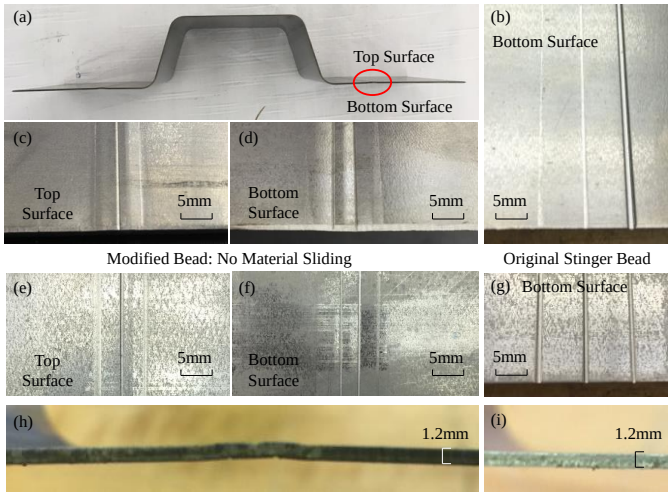

Figure 7 Stamped U-channel part with post-stretching process. (a) Side view of the sprung U-channel with an effective post-stretching amount larger and equal to 7mm for both 1.2mm DP980 and CP1180, using the modified bead. The marked area is magnified in the rest of subfigures. (b) The bottom surface of the bead area, using 1.2mm DP980 and the original stinger bead with a clamping force of 0.1Ton/mm. (c) and (d) Top and bottom surfaces of the bead area, respectively, using the modified bead under the same scenario. (e) and (f) Same as (c) and (d), respectively, with 1.2mm CP1180 under a clamping force of 0.175Ton/mm. (g) Same as (b), with 1.2mm CP1180 under a clamping force of 0.35Ton/mm. (h) and

(i) side views of the bead area for 1.2mm DP980 under a clamping force of 0.1Ton/mm, using the modified and original beads, respectively.

4.3. Hybrid Bead and Its Mechanism

The experimental results give a good insight of the modified bead forming mechanism, as a counterpart of the simulation results in the previous section. Its bead forming includes two different patterns, a) material penetration by the sharp teeth, and b) waved-shape forming by the specific teeth arrangement. Both the indented teeth and the edges of the wave shape synergistically contribute to restrict material flow in that area. The optimized bead can then be renamed as "hybrid" bead, related to its mechanism. A small amount of post-stretching will be given after fully engagement, which induces strong plastic deformation to dominate the spring-back related elastic counterpart. The existed lock beads, either a stinger-typed bead or conventional draw bead, do not possess the described synergistic mechanisms of material locking. The hybrid bead combines both the advantages of stinger-typed bead and conventional draw bead, by a) bilaterally applying the material penetration force between both sides of the blank and b) generate a relatively shallow but effective waved-shaped corrugation to block the material flow.

5. Analytical Solution of Spring-back

An analytical model is developed for predicting the U-channel spring-back shape with post-stretching process. The model directly implements the material constitutive relationship to analytically compute the stress-strain statuses through the thickness, for different regions in the U-channel cross-section. The details of the model are described in another proceeding publication. The model input includes material card (hardening behavior), geometrical factors and post-stretching forces. The last one, specifically, can be indirectly obtained by the punch force from press machine individually for each case.

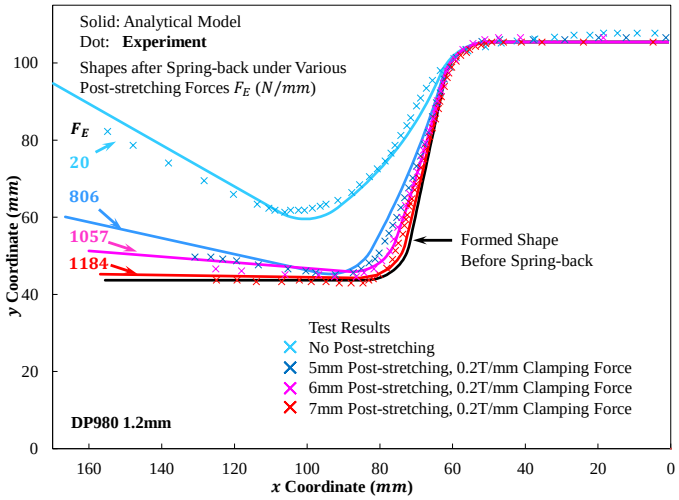

Figure 8 Comparison between experimental and analytically predicted sprung-back shapes for 1.2mm DP980. The predicted results are very close to the tested ones.

Figure 8 and compares the analytically predicted sprung-back shapes to the testes ones, which are digitally sketched. It can be seen that the predictions are very well correlated to the experimental ones for every case. A slight bulge can be observed in the experimental results between the punch radius and sidewall zones, especially under insufficient stretching forces. This is due to the gap between the die and punch surface, liberating a shred amount of material from contacting to the tool. This specific area is then free from bending and appears as a straight line segment. It would remain straight when no or weak post-stretching force is applied, generating the bulge. This is a local behavior that is not considered in the analytical solution, and does not significantly affect the spring-back results.

6. Conclusions

A post-stretching process is developed and implemented in a U-channel stamping die. The spring-back behavior, including angular opening and sidewall curl, can be effectively controlled. An innovatively designed hybrid bead is applied in the post-stretching process. Cross-sectional FE simulations are conducted to assist the bead design optimization, using DP980 AHSS. A comprehensive study is conducted to investigate the effects of both post-stretching amount and clamping force. Experimental results show excellent spring-back controlling performance using 1.2mm DP980 and CP1180 AHSSs. The tonnage can then be significantly reduced. An analytical solution is also applied to predict the spring-back shapes, correlating very well with the experimental results.

Acknowledgments

The authors gratefully acknowledge supports from AK Steel, General Motors Corporation, and Auto Steel Partnership (A/SP) stamping team. Especially, the authors gratefully acknowledge the significant contributions of Dr. Changqing Du and Dr. Dajun Zhou of Fiat Chrysler Automobiles for their active participations and many helpful suggestions.

References

[1] Marciniak Z, Duncan J L and Hu S J 2002 *Mechanics of sheet metal forming* (Butterworth-Heinemann)
[2] Semiatin S L, Marquard E and Lampman H 2006 *ASM Handbook, Volume 14B: Metalworking: Sheet Forming* ed S L Semiatin, E Marquard and H Lampman (ASM International)
[3] Wagoner R H, Lim H and Lee M G 2013 Advanced issues in springback *Int. J. Plast.* **45** 3–20
[4] Panthi S K, Ramakrishnan N, Pathak K K and Chouhan J S 2007 An analysis of springback in sheet metal bending using finite element method (FEM) *J. Mater. Process. Technol.* **186** 120–4
[5] Andersson A 2007 Numerical and Experimental Evaluation of Springback in Advanced High Strength Steel *J. Mater. Eng. Perform.* **16** 301–7
[6] Mori K ichiro, Abe Y and Suzui Y 2010 Improvement of stretch flangeability of ultra high strength steel sheet by smoothing of sheared edge *J. Mater. Process. Technol.*
[7] Mullan H B 2004 Improved prediction of springback on final formed components *J. Mater. Process. Technol.* **153** 464–71
[8] Lee M-G, Kim D, Kim C, Wenner M L and Chung K 2005 Spring-back evaluation of automotive sheets based on isotropic–kinematic hardening laws and non-quadratic anisotropic yield functions, part III: applications *Int. J. Plast.* **21** 915–53
[9] Gomes C, Onipede O and Lovell M 2005 Investigation of springback in high strength anisotropic steels *J. Mater. Process. Technol.* **159** 91–8
[10] Takamura M, Fukui A, Yano H, Hama T, Sunaga H, Makinouchi A and Asakawa M 2011 Investigation on Twisting and Side Wall Opening Occurring in Curved Hat Channel Products Made of High Strength Steel Sheets pp 887–94
[11] Takamura M, Sakata M, Fukui A, Hama T, Miyoshi Y, Sunaga H, Makinouchi A and Asakawa M 2010 Investigation of twist in curved hat channel products by elastic-plastic finite element analysis *Int. J. Mater. Form.* **3** 131–4
[12] Yen Y C, Jain A and Altan T 2004 A finite element analysis of orthogonal machining using different tool edge geometries *J. Mater. Process. Technol.* **146** 72–81
[13] Pu C and Gao Y 2015 Crystal Plasticity Analysis of Stress Partitioning Mechanisms and Their Microstructural Dependence in Advanced Steels *J. Appl. Mech.* **82** 31003
[14] Jia Y and Bai Y 2016 Ductile fracture prediction for metal sheets using all-strain-based anisotropic eMMC model *Int. J. Mech. Sci.* **115**–**116** 516–31
[15] Pu C, Gao Y, Wang Y and Sham T-L 2017 Diffusion-coupled cohesive interface simulations of stress corrosion intergranular cracking in polycrystalline materials *Acta Mater.* **136** 21–31
[16] Sun Z, Song G, Sisneros T A, Clausen B, Pu C, Li L, Gao Y and Liaw P K 2016 Load

partitioning between the bcc-iron matrix and NiAl-type precipitates in a ferritic alloy on multiple length scales *Sci. Rep.* **6** 1–9
[17] Ueda M, Ueno K and Kobayashi M 1981 A study of springback in the stretch bending of channels *J. Mech. Work. Technol.* **5** 163–79
[18] Ayres R A 1984 SHAPESET: A process to reduce sidewall curl springback in high-strength steel rails *J. Appl. Metalwork.* **3** 127–34
[19] Huang M 2007 Springback Control For DP590 S-Rail : Design & Application Better formability More Springback *Great Designs in Steel*
[20] Zhou D, Du C, Hsiung C, Schmid K, Ren F and Liasi E 2016 UHSS Springback Reduction with Post-Stretch *The IDDRG 2016 Conference Proceedings* (Linz, Austria)
[21] Stevenson R 1993 Springback in simple axisymmetric stampings *Metall. Trans. A* **24** 925–34